LIMIT CYCLING IN OBSERVER-BASED CONTROLLED MECHANICAL SYSTEMS WITH FRICTION

D. Putra [*], **H. Nijmeijer**[§]

Department of Mechanical Engineering, Eindhoven University of Technology
P.O. Box 513, 5600 MB Eindhoven, The Netherlands.
Fax +31 40 246 1418, Phone +31 40 247 [*]4850/[§]3203
E-mail: [*]d.putra@tue.nl, [§]h.nijmeijer@tue.nl

Keywords: limit cycle, friction compensation, observer, bifurcation, discontinuous system.

Abstract

In this paper, it is shown that observer-based controlled mechanical systems with friction may exhibit limit cycling. The limit cycling is induced by the interaction between friction and friction compensation, which is based on the estimated velocity. This limit cycling phenomenon, which is experimentally observed in a rotating arm manipulator, is analyzed through the shooting method and bifurcation analysis. The numerical results match well with laboratory experiments. The bifurcation analysis confirms that the limit cycling can be eliminated by enlarging the controller gains and the observer gains at the cost of a steady state error.

1 Introduction

Friction occurs in all mechanical systems, e.g. bearings, servo systems, and robotic manipulators [2, 3, 12]. In motion controlled systems, friction can severely deteriorate systems performance in terms of tracking errors, large steady state errors, and limit cycling oscillations. It is therefore important to understand friction phenomena and know how to deal with them in order to improve the systems performance. The availability of precise experimental observations has been a good driving force for investigations of friction models and compensation techniques of friction [2, 3, 5, 12]. Good matching between experimental observations and theoretical results is an important aspect in these investigations.

In positioning control systems, limit cycling is an undesired phenomenon due to its oscillatory and persistent behavior. Friction induced limit cycling has been investigated in many papers for examples see [1, 2, 9, 13, 16] and references therein. Most of these papers investigate stick-slip limit cycling in PID controlled systems. However, there is still a gap between theoretical results and practical observations; the disappearance of the stick-slip limit cycle by properly tuned PID controllers in industrial applications is not yet well understood. Recently, Hensen [9] confirmed through computational bifurcation methods the disappearance of the limit cycle for certain settings of a PID controller and some friction models. Limit cycling in a flexible servo system is another friction induced limit cycling that has been investigated, see e.g. [4, 19]. In this case, the interaction between friction and the flexible mode of the system play an important role for the occurrence of the limit cycle. This type of friction induced limit cycling is far from fully being understood. According to the survey paper of Armstrong et al. [2] and a recent literature study, limit cycling that is induced by the interaction between friction and friction compensation, which is based on estimated velocities in observer-based controlled systems with friction has not been documented yet. Nevertheless, we observe this limit cycling phenomenon experimentally in a rotating arm manipulator, so further study is required.

Observer-based positioning control systems with friction are of interest for the following reasons. In practical applications positioning control mechanical systems, such as robotic manipulators, are not equipped with velocity sensors for reasons as e.g. savings in cost, volume and weight that can be obtained. On the other hand, friction is often understood as a function of the velocity so that for friction compensation velocity signals are needed. Thus, we need to design observers in order to obtain velocity signals form the available position measurements and use them for friction compensation. Unfortunately, most of the available compensation techniques for friction, for example see [2, 3, 5, 12], require the actual velocity signal. Some authors have already addressed problems of friction compensation based on estimated velocity, see e.g. [7, 18]. In this case, a very simple friction model is considered, which is a constant times the sign of velocity, and no limit cycling result has been reported.

We analyze limit cycling in an observer-based controlled positioning system with friction through numerical methods using the shooting method and computational bifurcation analysis [10, 14]. Experimental validation is obtained from a rotating arm manipulator. The computed bifurcation diagram shows some bifurcations of limit cycles including a fold bifurcation where limit cycles disappear after the bifurcation point, which is interesting for a control purpose to eliminate limit cycling. In this case, we use a switch friction model, which is used in [9, 10]. This switch friction model, which can be considered as an extension of the Karnopp friction model, is a static friction model that consists of static friction, Coulomb friction, Stribeck curve, and viscous friction. Leine et al. [10] show that the switch friction model does not have any numerical instability problem in the stick phase as the Karnopp friction

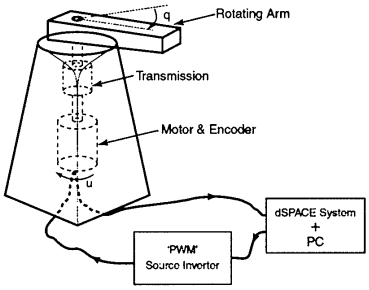

(a) The rotating arm system

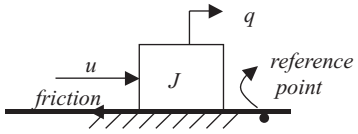

(b) Schematic diagram of the system

Figure 1: The experimental setup

model has, and it is computationally efficient compared to the smoothed friction model. The ability of the shooting method to analyse stick-slip limit cycles induced by the switch friction model has been demonstrated in [9, 10]. Since the shooting method finds a limit cycle or a periodic solution of nonlinear systems in general by solving a two-point boundary-value problem, it can also find other types of friction induced limit cycles of the switch friction model.

This paper is organized as follows. Section 2 introduces the system of interest: the experimental setup, its model and the observer-based controller scheme. In section 3, we discuss two characteristics of the closed loop system; the equilibrium set is discussed in subsection 3.1 and the dynamics of the switching surfaces is discussed in subsection 3.2. Section 4 consists of three subsections: subsection 4.1 introduces limit cycling behavior of the controlled setup, subsection 4.2 presents simulation results and validation of the model, and subsection 4.3 analyzes limit cycles of the controlled system using the shooting method. In section 5, we discuss computational bifurcation analysis to verify the disappearance of limit cycles, and we give some experimental validation of the bifurcation phenomena. Finally, conclusions and future research are given in section 6.

2 Experimental Setup

The experimental setup is a rotating arm manipulator consisting of an induction motor, a planetary transmission, and a rotating arm; which is depicted in Figure 1(a). Due to bearings and seals in the motor and in the transmission, the inertia of the total system, i.e. the combined inertia of the separate elements, is subject to friction. The system is controlled using a PC with a dSPACE system [6]. During the experiment the sampling frequency of the dSPACE is set to 5 *khz*, and the angular displacement of the rotating arm is measured using an encoder with accuracy 3.84×10^{-5} *rad*.

3 Modelling and Control

The rotating arm system with a regulation task can be considered as a system of a block mass that is moved by a control force to a desired position on a surface with friction, see Figure 1(b). In figure 1(b), J is the inertia of the block, q its position measured with respect to some reference point, and u the control force. The dynamics of the block are given as

$$\dot{x} = Ax - Bf(x,u) + Bu \quad (1)$$
$$y = Cx \quad (2)$$

where $x = \begin{bmatrix} x_1 & x_2 \end{bmatrix}^T$ is the state with x_1 and x_2 the position and the velocity of the block respectively, $A = \begin{bmatrix} 0 & 1 \\ 0 & -D/J \end{bmatrix}, B = \begin{bmatrix} 0 \\ 1/J \end{bmatrix}$, with D the damping coefficient of the viscous friction, f is the nonlinear friction,$C = \begin{bmatrix} 1 & 0 \end{bmatrix}$, and y is the measured position. The nonlinear friction is given by a switch model [10]

$$f(x,u) = \begin{cases} g(x_2)sign(x_2) & if\,|x_2| > \eta \\ u & if\,|x_2| \le \eta\, and\, |u| \le F_s \\ F_s sign(u) & otherwise \end{cases} \quad (3)$$

where $g(x_2) = F_c + (F_s - F_c)e^{-(x_2/v)^2}$ is the Stribeck curve with F_c the Coulomb friction level, $F_s > F_c$ the static friction level, and v the Stribeck velocity; and $\eta << 1$ is a narrow band around zero velocity that is introduced to overcome computational instability at zero velocity. The narrow band η is chosen such that $Tol < \eta << 1$, where Tol is the tolerance of the integration method, and in the ideal case $\eta = 0$. Applying the switch friction model (3) to the state space (1), in the stick phase the system is governed by

$$\dot{x}_1 = x_2 \quad (4)$$
$$\dot{x}_2 = \frac{-D}{J}x_2. \quad (5)$$

In this way, the acceleration in the stick phase is not immediately set to zero as in the Karnopp model, instead it is continuously forced to zero by using the linear viscous friction. This

Parameter	Value
$J[kg.m^2]$	0.0260
$D[N.m.s/rad]$	0.0710
$F_c[N.m]$	0.4195
$F_s[N.m]$	0.5005
$v_s[rad/s]$	0.15

Table 1: Parameter values of the rotating arm setup

term maintains the continuity of the velocity and thus avoids numerical instability problems in the stick phase.

Parameter values of the setup for the derived model are given in Table 1. The inertia parameter J is obtained from a Bode plot and the friction parameters are obtained by fitting a curve to the friction-velocity map, i.e. the averaged input torques at different constant velocities, that minimizes the quadratic cost function

$$\min_{\theta} \sum_{k=1}^{M} [f_{ss}(\dot{q}_k) - f(\dot{q}_k, \theta)]^2 \tag{6}$$

where $f_{ss}(\dot{q}_k)$ is the average input torque during a constant velocity $\dot{q}_k$, $\theta = [\ D \quad F_s \quad F_c \quad v_s\ ]$ is a vector containing all friction parameters, and M is the number of data points [9].

In order to regulate the block mass at a desired position y_d, we consider a linear output feedback with friction compensation of the form

$$u = \bar{u} + \hat{f}(\hat{x}, \bar{u}) \tag{7}$$

where $\bar{u} = N(\hat{x} - x_d)$ with $N = [\ n_1 \quad n_2\ ]$ the controller gain, $x_d = [\ y_d \quad 0\ ]^T$ the desired state, $\hat{x}$ the estimated state that is obtained from an observer, and $\hat{f}$ is the nonlinear friction compensation. Without loss of generality, we assume that the desired position is the origin, hence

$$u = N\hat{x} + \hat{f}. \tag{8}$$

Consider an observer of the form

$$\dot{\hat{x}} = A\hat{x} - B\hat{f} + Bu + L(y - \hat{y}) \tag{9}$$

where $L = [\ l_1 \quad l_2\ ]^T$ is the observer gain. Substitution of (8) into (9) results a linear observer

$$\dot{\hat{x}} = (A - LC + BN)\hat{x} + LCx. \tag{10}$$

This is an advantage of using feedback to compensate friction. Rearranging the system (1) and (2) with the control law (8) and the observer (10) yields the closed loop system

$$\begin{bmatrix} \dot{x} \\ \dot{\hat{x}} \end{bmatrix} = \begin{bmatrix} A & BN \\ LC & A - LC + BN \end{bmatrix} \begin{bmatrix} x \\ \hat{x} \end{bmatrix} + \begin{bmatrix} B \\ 0 \end{bmatrix} (\hat{f} - f). \tag{11}$$

Since the pair (A, B) is controllable and the pair (C, A) is observable, we can assign separately poles for the controller and poles for the observer in order to make the linear part of the closed loop system exponentially stable [15]. The controller poles and the observer poles are given by eigenvalues of the matrices $A + BN$ and $A - LC$ respectively. We only consider controller gains and observer gains with stable poles.

4 Equilibrium Set

Since we consider a regulation task, it is important to realize that the desired position belongs to the equilibrium set of the controlled system. The equilibrium set of the controlled system (11) is obtained by setting $\dot{x} = 0$ and $\dot{\hat{x}} = 0$. Thus, the equilibrium set is given by

$$\bar{\xi} = \left\{ \begin{array}{c} (\bar{x}, \bar{\hat{x}}) | \bar{x}_1 = \frac{Jl_2 + Dl_1 - n_2 l_1 - n_1}{n_1 l_1} \bar{\hat{x}}_2, \bar{\hat{x}}_1 = \frac{Jl_2 + Dl_1 - n_2 l_1}{n_1 l_1} \bar{\hat{x}}_2, \\ \bar{x}_2 = 0, -F_s \leq (\frac{Jl_2}{l_1} + D)\bar{\hat{x}}_2 + \hat{f}(\bar{\hat{x}}_2) \leq F_s \end{array} \right\}. \tag{12}$$

It is trivial that the origin, the desired state, belongs to equilibrium set (12). Since the size of the equilibrium set (12) depends on solutions of the inequality constraint of $\hat{x}_2$, it can be manipulated by tuning the observer gains l_1 and l_2. It is important to realize that the size of this equilibrium set gives the boundary of the possible steady state errors.

5 Limit Cycling Behavior

In this section, we investigate limit cycling behavior of the controlled system (11). Firstly, we present some experimental results of the controlled setup for some sets of controller gains N and observer gains L. Secondly, simulations results are presented in order to see the ability of the model to mimic the dynamics of the experimental setup. At the end of this section, limit cycles of the model are analyzed using the shooting method and the results are compared with experimental observations.

5.1 Experimental Results

The response of the controlled setup with the controller gain $N = [\ -0.26 \quad -0.06\ ]$, the observer gain $L = [\ 2.3077 \quad 1.4793\ ]^T$, and initial conditions $x(0) = [\ 3.1 \quad 0\ ]^T$, and $\hat{x}(0) = [\ 3 \quad 0\ ]^T$ is shown in Figure 2. For these gains the controller poles and the observer poles are located at $-2.519 \pm 1.911i$ and $-2.519 \pm 1.198i$, respectively.

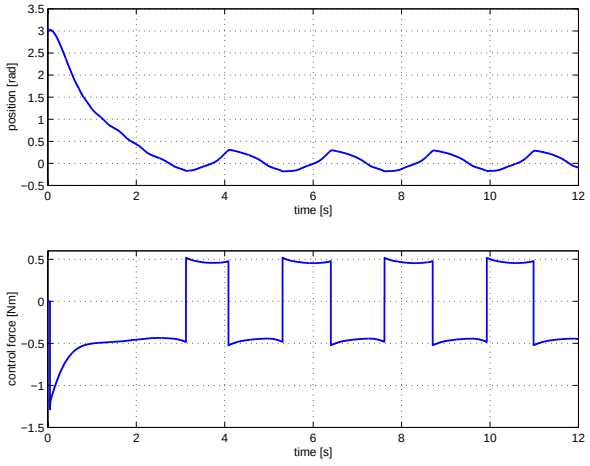

Figure 2: Response of the setup for smaller gains

Controller poles	Observer poles	Limit cycle	
		Amplitude	Period
$-2.519 \pm 1.911i$	$-2.519 \pm 1.198i$	$0.2025rad$	$2.3345s$
$-2.519 \pm 1.911i$	$-6.519 \pm 1.260i$	$0.1801rad$	$1.1247s$
$-7.00 \pm 3.00i$	$-6.519 \pm 1.260i$	$0.0380rad$	$0.7839s$
$-7.00 \pm 3.00i$	$-12.00 \pm 4.00i$	$0.0347rad$	$0.7809s$

Table 2: Limit cycling of the controlled setup

Figure 2 shows that the controlled setup exhibits limit cycling around the desired position. Limit cycling of the controlled setup for some sets of gains are summarized in Table 2. Since the poles give a qualitative feature of the gains, we represent the gains by the corresponding poles. Notice that larger gains correspond to faster poles. Table 2 shows that both the amplitude and the period of the limit cycle decrease as the controller gain and the observer gain increase, i.e. the poles become faster. If we enlarge the gains to $N = [\ -3.016 \quad -0.449\ ]$ and $L = [\ 21.2677 \quad 101.8901\ ]^T$ such that the controller poles and the observer poles are located at $-10 \pm 4i$ and $-12 \pm 4i$ respectively, the controlled setup does not exhibit limit cycling anymore. The response of the controller setup for this set of gains is depicted in Figure 3; a steady state error appears which in this case equals $2.3 \times 10^{-4}\ rad$. If we repeat the experiment with different initial conditions, we may end up at a different steady state error.

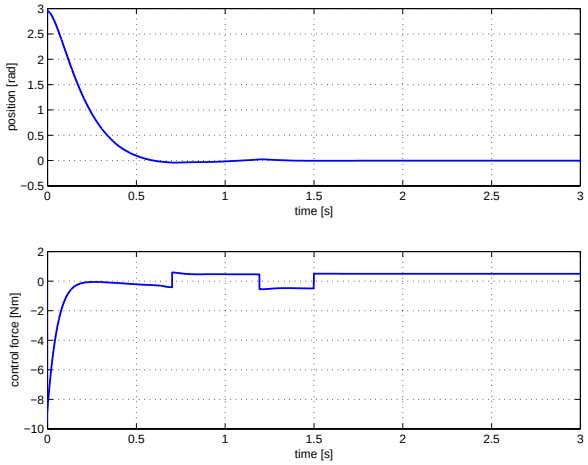

Figure 3: Response of the setup for larger gains

5.2 Simulation results and model validation

In order to validate the model derived in section 3, some simulations are carried out in $Matlab^{TM}$ using the integration routine *ode45* with the integration tolerance $Tol = 10^{-9}$ and $\eta = 10^{-5} rad/s$. Comparison between the responses of the model and the experimental setup with $N = [\ -0.26 \quad -0.06\ ]$, $L = [\ 2.3077 \quad 1.4793\ ]^T$, $x(0) = [\ 3.1 \quad 0\ ]^T$, and $\hat{x}(0) = [\ 3 \quad 0\ ]^T$ are depicted in Figures 4(a) and 4(b). These figures show that limit cycle of the model matches well with the limit cycle of the experimental setup. Simulation results also confirm the disappearance of the limit cycle, which is observed in the experimental setup, if we enlarge the gains to $N = [\ -3.016 \quad -0.449\ ]$ and $L = [\ 21.2677 \quad 101.8901\ ]^T$. The steady state error of a simulation result is $1.57 \times 10^{-6}\ rad$, where the one obtained in the experimental setup is $2.3 \times 10^{-4}\ rad$. According to the equilibrium set (12), the steady state error is bounded by $|e_{x_1}| \leq 2.6 \times 10^{-6}\ rad$. A larger steady state error of the experimental result is due to the resolution of the position measurements of $3.84 \times 10^{-6}\ rad$ and the exact nature of the friction that is not captured by the friction model (3).

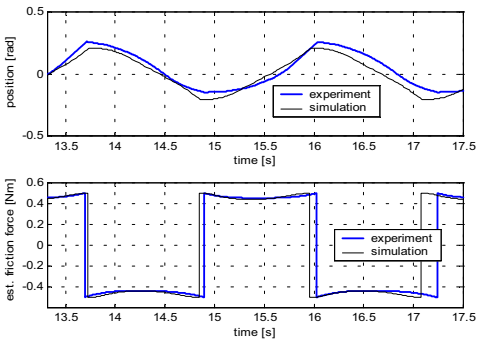

(a) Time series

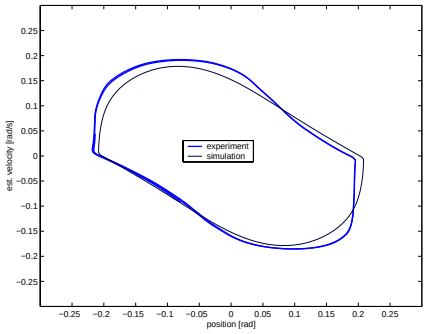

(b) Projection on a phase plane

Figure 4: Limit cycles of the controlled setup and the model

5.3 Numerical analysis of limit cycles

A limit cycle of the controlled system (11), if it exists, can be computed by solving a two-point boundary-value problem given by the periodic nature of the limit cycle. Let $\phi_t(\xi_0)$

denotes the solution of the controlled system (11) at time t initialized at $t = 0$ in ξ_0, where $\xi = \begin{bmatrix} x & \hat{x} \end{bmatrix}^T$. Since a limit cycle γ is a periodic solution of the (11), then

$$\phi_T(\xi_\gamma) - \xi_\gamma = 0 \tag{13}$$

holds, where T is the period time of the limit cycle and $\xi_\gamma \in \gamma$ is point on the limit cycle. Equation (13) defines a two-point boundary-value problem with unknowns T and ξ_γ related to a limit cycle of the controlled system (11). A popular algorithm to solve this two-point boundary-value problem, which can handle the discontinuous friction model (3), is the shooting method. The shooting method is an iterative scheme, which is similar to the Newton-Raphson algorithm, for details see [10, 14]. The stability of a limit cycle is determined by its Floquet multipliers, which are eigenvalues of the monodromy matrix [8]. The monodromy matrix is the transition matrix of the linearization around a periodic solution after one period time. Since the controlled system (11) is discontinuous, the associated monodromy matrix is obtained from a sensitivity analysis as proposed in [10]. This monodromy matrix is used in the shooting method to find a limit cycle and to determine its stability. Results of the shooting method are summarized in Table 3. The numerical results in Table 3 are comparable to the experimental results in Table 2. These results of the shooting method confirm stability of all limit cycles, which are obtained in the experimental setup.

6 Bifurcation of Limit Cycles

Both experimental results and numerical results show that the amplitude and the period time of the limit cycle decrease if we make the controller poles and the observer poles faster, and eventually the limit cycle disappears at some faster poles. It is of interest to study bifurcations of limit cycles to verify these results. For this purpose, the controller gain N and the observer gain L are parameterized by a single parameter r such that the poles of the controller and the observer are given by $s_c = -\frac{r}{2} \pm \frac{r\sqrt{3}}{2}i$ and $s_o = -\frac{\alpha r}{2} \pm \frac{\alpha r\sqrt{3}}{2}i$, respectively. Since $|s_c| = r$ and $|s_o| = \alpha r$, the parameter r is essentially the distance of the controller poles from the origin and α is a scaling factor for the distance of the observer poles. Using this parametrization the controller gain is given by $N = \begin{bmatrix} -Jr^2 & D - Jr \end{bmatrix}$, and the observer gain is given by $L = \begin{bmatrix} \alpha r - D/J & (\alpha r - D/J)D/J + \alpha^2 r^2 \end{bmatrix}^T$. In this case, we choose $\alpha = 1.2$ in order to make the observer poles faster than the controller poles. Possible bifurcations of the limit cycle will be investigated with respect to variation of the design parameter r. We use the pseudo-arclength continuation method [14, 17] in combination with the shooting method to trace the branches of limit cycles. A bifurcation point of limit cycles is obtained when one Floquet multiplier (or a pair of them) passes through the unit circle and one or more branches of limit cycles may appear or disappear around the bifurcation point [11, 17, 8].

The computed bifurcation diagram of limit cycles of the controlled system for $2.5 \leqslant r \leqslant 19$ is depicted in Figure 5. The

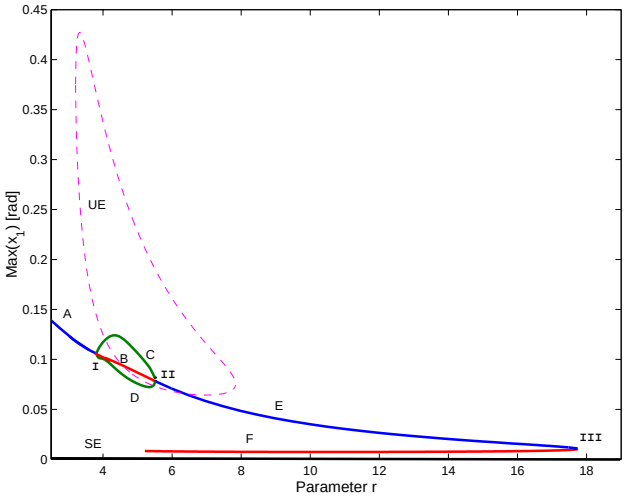

Figure 5: Bifurcation diagram of the controlled system

vertical axis in Figure 5 is the peak value of the limit cycle. The bifurcation diagram show six branches of limit cycles: A is a branch of stable symmetric limit cycles with two sticking events,i.e. the rotating arm sticks twice in one cycle, B and F are branches of unstable symmetric limit cycles without sticking event, C and D are branches of stable asymmetric limit cycles with one sticking event, and E is a branch of stable symmetric limit cycles without sticking event. The bifurcation diagram also show two equilibrium sets: SE is a stable equilibrium set and UE is an unstable equilibrium set. There should be another equilibrium set, which is the mirror of UE, due to the symmetrical friction model, see the equilibrium set (12).

In the bifurcation diagram, we observe three bifurcations of limit cycles. At the bifurcation point I, the symmetric branch A becomes unstable, which creates the unstable branch B, and two branches of asymmetric limit cycles, C and D that are mirror of each other, are created. At this bifurcation point the symmetric branch not only looses its stability but it also looses the sticking mode. This bifurcation could be called a "discontinuous symmetry-breaking" bifurcation [11]. The symmetric branch E looses its stability at the bifurcation point II and two branches of asymmetric limit cycles, C and D, appear. A this bifurcation point the symmetric branch does not gain or loose any sticking mode, this bifurcation is called a "symmetry-breaking" bifurcation. At the bifurcation point III, the stable branch E collides with the unstable branch F and then they disappear after the bifurcation point. This type of bifurcation is called a fold bifurcation. Thus, the bifurcation diagram confirms the disappearance of limit cycles at some faster poles of the controller and the observer. Notice that the larger r the faster the poles are.

7 Conclusions and Future Research

The limit cycling phenomena in observer-based controlled systems with friction, which are experimentally observed in a

Controller poles	Observer poles	Limit cycle		
		Amplitude	Period	Stability
$-2.519 \pm 1.911i$	$-2.519 \pm 1.198i$	$0.2082rad$	$2.2292s$	stable
$-2.519 \pm 1.911i$	$-6.519 \pm 1.260i$	$0.1524rad$	$1.8541s$	stable
$-7.00 \pm 3.00i$	$-6.519 \pm 1.260i$	$0.0527rad$	$0.8915s$	stable
$-7.00 \pm 3.00i$	$-12.00 \pm 4.00i$	$0.0484rad$	$0.8363s$	stable

Table 3: Analysis of limit cycles using the shooting method

rotating arm system, have been analyzed using the shooting method and computational bifurcation analysis. The numerical results match well with the experimental observations. The limit cycling appears to exhibit "discontinuous symmetry-breaking", "symmetry-breaking", and fold bifurcations. The bifurcation analysis confirms that the limit cycling can be suppressed and eventually eliminated by making controller poles and observer poles faster, i.e. enlarging the controller gains and the observer gains. Further work is needed to derive a design procedure for controller gains and observer gains, which guarantees that the closed loop system does not exhibit limit cycling. The current result suggests that the design procedure can be based on an accurate prediction of a fold bifurcation point.

Acknowledgment

The work in this paper was partly supported by the European Project SICONOS 2001-37172.

References

[1] B. Armstrong-Hélouvry and B. Amin. Pid control in the presence of static friction: A comparison of algebraic and describing function analysis. *Automatica*, 32:679–692, 1996.

[2] B. Armstrong-Hélouvry, P. Dupont, and C. Canudasde-Wit. A survey of models, analysis tools, and compensation methods for the control of machines with friction. *Automatica*, 30:1083–1138, 1994.

[3] B. Armstrong-Hélouvry. *Control of Machines with Friction*. Kluwer Academic Publishers, 1991.

[4] A. Bonsignore, G. Ferretti, and G. Magnani. Coulomb friction limit cycles in elastic positioning systems. *ASME Journal of Dynamics Systems, Measurement, and Control*, 121:298–301, 1999.

[5] C. Canudas de Wit, H. Olsson, K. J. Åström, and P. Lischinsky. A new model for control of systems with friction. *IEEE Transaction on Automatic Control*, 40:419–425, 1995.

[6] dSPACE. *DS1102 User's Guide*. dSPACE digital signal processing and control engineering GmbH, 1999.

[7] B. Friedland and S. Mentzelopoulou. On adaptive friction compensation without velocity measurement. In *Proceeding of the 1st IEEE Conference on Control Applications*, pages 1076–1081, Dayton, OH, 1992.

[8] J. Guckenheimer and P. Holmes. *Nonlinear Oscillations, Dynamic Systems, and Bifurcation of Vector Fields*. Springer, 1983.

[9] R. H. A. Hensen. *Controlled Mechanical Systems with Friction*. PhD thesis, Endhoven University of Technology, The Netherlands, 2002.

[10] R. I. Leine, D. H. van Campen, A. de Kraker, and L. van den Steen. Stick-slip vibrations induced by alternate friction models. *Nonlinear Dynamics*, 16:41–54, 1998.

[11] R. I. Leine. *Bifurcations in Discontinuous Mechanical Systems of Filippov-Type*. PhD thesis, Endhoven University of Technology, The Netherlands, 2000.

[12] H. Olsson, K. J. Åström, C. CanudasdeWit, M. Gäfvert, and P. Lischinsky. Friction models and friction compensations. *European Journal of Control*, 4:176–195, 1998.

[13] H. Olsson and K. J. Åström. Friction generated limit cycles. In *Proceeding of the 1996 IEEE Conference on Control Applications*, pages 798–803, Dearborn, MI, 1996.

[14] T. S. Parker and L. O. Chua. *Practical Numerical Algorithms for Chaotic Systems*. Springer-Verlag, 1989.

[15] J. W. Polderman and J. C. Willems. *Introduction to Mathematical Systems Theory: A Behavioral Approach*. Springer, 1998.

[16] C. J. Radcliffe and S. C. Southward. A property of stick-slip friction models which promotes limit cycle generation. In *Proceeding of the 1990 American Control Conference*, pages 1198–1203, San Diego, CA, 1990.

[17] R. Seydel. *Practical Bifurcation and Stability Analysis: From Equilibrium to Chaos*. Springer-Verlag, 1994.

[18] S. Tafazoli, C. W. de Silva, and P. D. Lawrence. Friction estimation in a planar electrohydraulic manipulator. In *Proceeding of the 1994 American Control Conference*, pages 3294–3298, Baltimore, MD, 1994.

[19] A. Wallenborg and K. J. Åström. Limit cycle oscillations in high performance robot drives. In *Proceeding of the 1988 International Conference on Control*, pages 444–449, U.K., 1988.